RNA Biology

ISSN: 1547-6286 (Print) 1555-8584 (Online) Journal homepage: http://www.tandfonline.com/loi/krnb20

Characterization of RNA binding and chaperoning activities of HIV-1 Vif protein

Dona Sleiman, Serena Bernacchi, Santiago Xavier Guerrero, Franck Brachet, Valéry Larue, Jean-Christophe Paillart & Carine Tisné

To cite this article: Dona Sleiman, Serena Bernacchi, Santiago Xavier Guerrero, Franck Brachet, Valéry Larue, Jean-Christophe Paillart & Carine Tisné (2014) Characterization of RNA binding and chaperoning activities of HIV-1 Vif protein, RNA Biology, 11:7, 906-920, DOI: 10.4161/rna.29546

To link to this article: http://dx.doi.org/10.4161/rna.29546

RESEARCH PAPER

RNA Biology 11:7, 906–920; Jul 2014; © 2014 Landes Bioscience

Characterization of RNA binding and chaperoning activities of HIV-1 Vif protein

Importance of the C-terminal unstructured tail

Dona Sleiman[1,†], Serena Bernacchi[2,†], Santiago Xavier Guerrero[2], Franck Brachet[1], Valéry Larue[1], Jean-Christophe Paillart[2,*], and Carine Tisné[1,*]

[1]Laboratoire de Cristallographie et RMN Biologiques; CNRS; Université Paris Descartes; Paris Sorbonne Cité; Paris, France; [2]Architecture et Réactivité de l'ARN; CNRS; Université de Strasbourg; Institut de Biologie Moléculaire et Cellulaire; Strasbourg, France

[†]These authors contributed equally to this work.

Keywords: HIV, Vif, RNA chaperone, nucleocapsid, unstructured domain

The viral infectivity factor (Vif) is essential for the productive infection and dissemination of HIV-1 in non-permissive cells, containing the cellular anti-HIV defense cytosine deaminases APOBEC3 (A3G and A3F). Vif neutralizes the antiviral activities of the APOBEC3G/F by diverse mechanisms including their degradation through the ubiquitin/proteasome pathway and their translational inhibition. In addition, Vif appears to be an active partner of the late steps of viral replication by interacting with $Pr55^{Gag}$, reverse transcriptase and genomic RNA. Here, we expressed and purified full-length and truncated Vif proteins, and analyzed their RNA binding and chaperone properties. First, we showed by CD and NMR spectroscopies that the N-terminal domain of Vif is highly structured in solution, whereas the C-terminal domain remains mainly unfolded. Both domains exhibited substantial RNA binding capacities with dissociation constants in the nanomolar range, whereas the basic unfolded C-terminal domain of Vif was responsible in part for its RNA chaperone activity. Second, we showed by NMR chemical shift mapping that Vif and NCp7 share the same binding sites on $tRNA^{Lys}_3$, the primer of HIV-1 reverse transcriptase. Finally, our results indicate that Vif has potent RNA chaperone activity and provide direct evidence for an important role of the unstructured C-terminal domain of Vif in this capacity.

Introduction

In addition to structural and enzymatic proteins essential for virus replication, the HIV-1 genome encodes six regulatory proteins (Tat, Rev, Nef, Vif, Vpr, and Vpu) that modulate virus fitness and infectivity in vivo. Among these proteins, Vif (Viral Infectivity Factor), a highly basic protein of 23 kDa, has been shown to be essential for viral pathogenesis by allowing HIV-1 replication in non-permissive cells, such as $CD4^+$ T lymphocytes and macrophages, the natural cell targets of the virus. In those cells, Vif neutralizes the cellular anti-HIV defense by interacting with cellular cytosine deaminases APOBEC3G (APOlipoprotein B mRNA-Editing enzyme-Catalytic, polypeptide-like 3G, or A3G) and A3F and inhibiting their antiviral activities.[1] In the absence of a functional Vif, A3G/3F proteins deaminate cytidines into uridines in the minus strand DNA[2-4] and inhibit reverse transcription and integration through deaminase-independent mechanisms.[5] Vif counteracts A3G/3F and allows HIV-1 replication by hijacking several cellular processes. First, Vif targets A3G/3F for degradation via the proteasome by recruiting an E3 ubiquitin ligase cellular complex composed of Elongin B (EloB), Elongin C (EloC), Cullin 5 (Cul5), and RING-box protein 2 (Rbx2).[6-8] CBF-β, the transcriptional Core Binding Factor-β, has recently been shown to be an integral component of this complex, directly interacting with Vif and favoring the specific polyubiquitination and degradation of A3G.[9-11] Second, Vif regulates A3G translation by binding to the 5′-UTR (untranslated region) of its mRNA, thus likely preventing its scanning by the ribosome.[12] These two mechanisms seem to be independent pathways utilized by Vif to reduce A3G expression,[13,14] and to indirectly interfere with its packaging.[15] In addition, Vif has been proposed to promote the assembly of A3G into presumably packaging-incompetent high molecular mass complexes.[16]

Vif consists of several functional and conserved domains (**Fig. 1**) (for reviews see refs. 17 and 18). The N-terminal domain (NTD) of Vif (residues 1–100) is enriched in hydrophobic amino acids, notably in conserved tryptophan residues. Mutagenesis studies have shown that these residues and other motifs/sequences are important for binding to A3G/3F,[19-22] but also to A3H, A3C, and A3DE.[23-25] In particular, NTD residues W11, Y30, and Y40 are important for Vif binding to RNA in vitro[26] and in infected cells.[27] Moreover, residues W21 and W38 are involved in binding

*Correspondence to: Carine Tisné; Email: carine.tisne@parisdescartes.fr; Jean-Christophe Paillart; Email: jc.paillart@ibmc-cnrs.unistra.fr
Submitted: 04/16/2014; Revised: 06/08/2014; Accepted: 06/10/2014; Published Online: 07/22/2014
http://dx.doi.org/10.4161/rna.29546

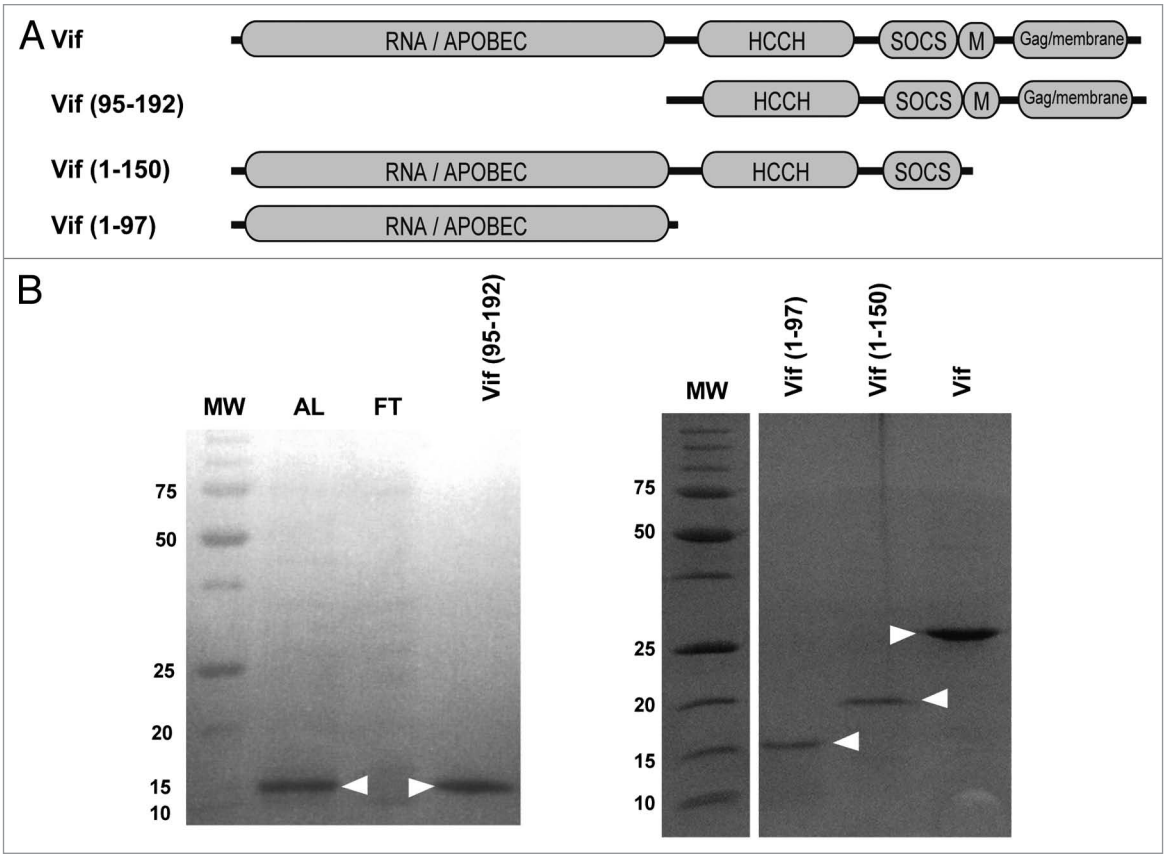

Figure 1. HIV-1 Vif and its domains. (**A**) Schematic representation of HIV-1 Vif functional domains and Vif constructions studied in this paper. HIV-1 Vif contains several functional domains, including an RNA/APOBEC3 binding domain, a conserved zinc-binding hydrophobic HCCH motif and a downstream SOCS-box, a multimerization domain (M) and a Gag/membrane binding domain. The number in parenthesis corresponds to the number of Vif amino acids encompassed in each construction. (**B**) SDS-PAGE analysis (14%) of purified Vif and its domains, on the left analysis of NiNTA purification of Vif (95–192) in denaturing condition, AL: after lysis of bacteria by denaturing lysis buffer, FT: analysis of the flow-through, Vif (95–192): analysis of the fractions of the NiNTA elution containing Vif (95–192) (see materials and methods). On the right, analysis of the other purified proteins studied in this paper. Proteins were visualized by Coomassie blue staining.

to CBF-β.[9,10,28] The central domain (residues 108–139) constitutes a non-consensus HCCH zinc-binding motif that binds Cul5.[29,30] Finally, the C-terminal domain (CTD) consists of (1) a SOCS-box motif (^{144}SLQ[Y/F]LAL^{150}) that promotes the interaction with EloC/EloB,[31] and is therefore important for the recruitment of the E3 ubiquitin ligase that targets A3G for degradation[32]; (2) an oligomerization domain (residues 151–164) containing a ^{161}PPLP^{164} motif critical for Vif oligomerization[33,34] and its interaction with the cellular kinase Hck[34,35]; and (3) a domain (residues 172–192) important for binding with Pr55^{Gag},[36,37] membranes,[38] and reverse transcriptase.[39]

Very recently, the structure of Vif in complex with CBF-β, Cul5 and EloB/C proteins was solved by X-ray crystallography.[40] The structure of Vif in the complex is maintained by extensive interactions with CBF-β, which binds to hydrophobic residues of Vif, leaving the positively charged surface exposed. In addition, Vif also interacts with Cul5 and EloC through two helices belonging respectively to the HCCH and BC-box domains. Although this structure explains how Vif can hijack the cellular proteasome degradation pathway, information on Vif interaction with APOBEC3 proteins and RNAs is still lacking. Alone in solution, Vif has been shown to be structurally unfolded,[41-43] and the disordered nature of the CTD is in line with secondary structure prediction models.[44] Moreover, conformational refolding of Vif has been observed upon self-oligomerization,[41] binding to EloC[45] and to specific RNA motifs such as the Trans-acting Responsive (TAR) element,[46,47] confirming the importance of unstructured regions in the multifunctional properties of Vif. Beside, direct analyses of Vif in cell by fluorescence techniques revealed the oligomerization of Vif through the C-terminal domain and the perturbation of this intrinsic property when Vif encounters binding partners such as APOBEC3G or Hck proteins.[18,48]

Vif has previously been shown to be an RNA binding protein with preferential binding to short RNA motifs present in the 5′ region of HIV-1 genomic RNA[46,49,50] as well as to A3G mRNA.[12,47] Moreover, Vif seems to participate to several important steps of the viral replication cycle such as reverse transcription,[51,52] and HIV-1 genomic RNA dimerization thanks to its RNA chaperone activity.[18,52] The basic and intrinsically disordered nature of HIV-1 Vif protein may account for its ability to interact with several other proteins and nucleic acids in a manner similar to RNA chaperones such as HIV-1 NCp7[53] and Tat[48] proteins or

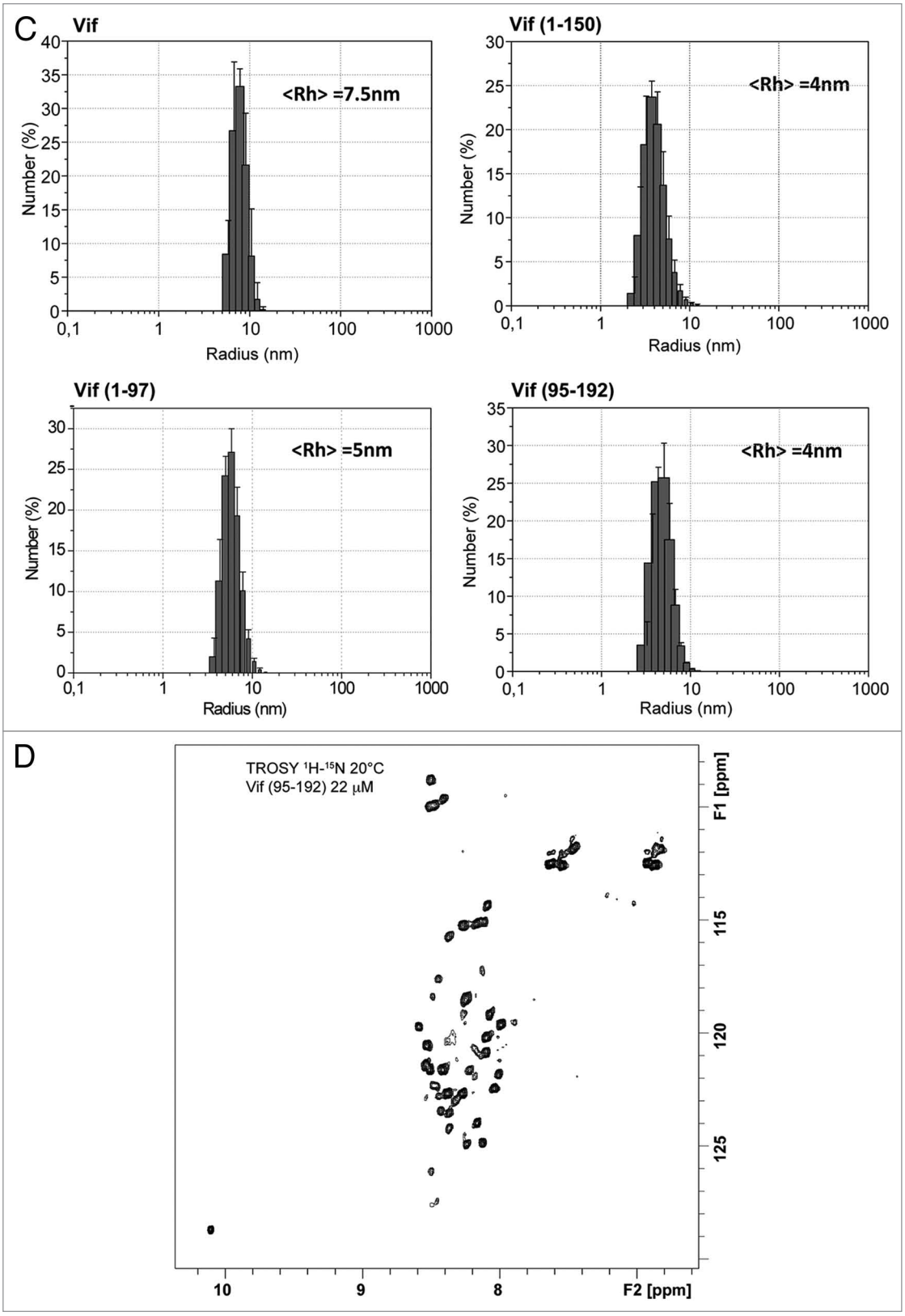

Figure 1. HIV-1 Vif and its domains. (**C**) Dynamic light scattering profiles of the HIV-1 Vif protein and its domains, Vif (1–150), Vif (1–97), Vif (95–192). The average hydrodynamic radius is indicated for each Vif protein domain. (**D**) ^{1}H-^{15}N TROSY NMR spectrum of Vif (95–192). The spectrum was recorded at 20 °C in the protein buffer.

Table 1. Analysis of CD spectra of Vif and its domains

Secondary structure Proteins	α-helix	β-strands	Random coils
Vif	15% (22%)	33% (26%)	52% (52%)
Vif (1–150)	2% (26%)	51% (31%)	47% (43%)
Vif (1–97)	25% (14%)	43% (45%)	32% (41%)
Vif (95–192)	20% (31%)	15% (5%)	65% (63%)

The data were fit using K2D software http://www.embl.de/~andrade/k2d.html.[86] Number in parenthesis shows the percentage of the secondary structure predictions by PSIPRED http://bioinf.cs.ucl.ac.uk/psipred/ calculated for each protein from the HIV-1 Vif protein prediction of its secondary structure.

the cellular fragile X mental retardation protein FMRP.[54] In this respect, the NTD of Vif was previously described to be responsible for its specific RNA binding affinity whereas the CTD, from residue 156 to 192, which contains many positively charged residues, could contribute to non-specific RNA binding.[26] To examine this possibility, we purified full-length and individual N- and C-terminal domains of HIV-1 Vif protein and analyzed their nucleic acid binding activities for a panel of RNAs. We also determined their oligomerization state and secondary structure elements in vitro. Moreover, we showed by NMR chemical shift mapping that Vif and NCp7 share the same binding sites on $tRNA^{Lys}_3$, with a joined participation of the NTD and CTD of Vif. Finally, we observed that Vif acts as chaperone by promoting efficient RNA annealing. Importantly our results provided direct evidence for an important role of the unstructured CTD of Vif in this capacity.

Results

Rational design of HIV-1 Vif domains and their purification

The subdomains of HIV-1 Vif protein (HXB2 isolate) studied in this work (**Fig. 1A**) were defined considering functional domains of Vif, solution conformation and dynamics of Vif obtained by mass spectrometry (MS),[42] NMR data on the CTD of Vif,[43] biochemical data regarding intrinsic proteolysis of Vif[55,56] and disorder prediction using various software tools.

First, it was shown that the NTD of Vif (residues 1–86) displayed the most protected region against amide exchange.[42,45] Consequently, this region is likely the most structured, in agreement with disorder prediction. Notably, the NTD of Vif contains a tryptophan-rich region that likely gives the protein the property to bind RNA.[26,46,50] Second, the CTD of Vif is predicted to be disordered, and this feature was actually demonstrated in solution by NMR and MS, either alone or in a full-length protein.[42,43] This domain includes the SOCS-box, the multimerization PPLP motif and the $Pr55^{Gag}$/membrane binding domain. Third, it has been noticed that Vif contains a specific cleavage site for the HIV-1 protease after residue 150, releasing a natural 1–150 degradation intermediate that is found not only in virions, but also in cells, and could thus reflect a co-packaging of this truncated form.[55,56] We did not study the corresponding peptide Vif (151–192) as we did not see any noticeable effects of this peptide on various HIV-1 replication steps (JC Paillart, unpublished results). We thus decided to work with three truncated version of Vif, namely Vif (1–97) ending up just after a predicted β-sheet secondary structure,[17] Vif (95–192) and Vif (1–150) and to compare their RNA binding and chaperone properties to that of full-length Vif protein.

Vif and its domains were overproduced in *E. coli* and purified in denaturing conditions as previously described.[42,44,46,47,50,52,57,58] It is known that recombinant Vif expressed alone in *E. coli* localizes to insoluble inclusion bodies. Vif in inclusion bodies can be isolated under denaturating conditions, purified by Ni-NTA affinity chromatography, and then refolded by subsequent dialysis with buffers containing decreasing concentrations of denaturant. The renaturing conditions for each domain were adjusted to optimize their solubility. A final concentration of 40 μmol/L for Vif (1–97) and Vif (95–192) and of 10 μmol/L for Vif and Vif (1–150) were obtained. The analysis by SDS-PAGE gel electrophoresis of purified Vif and its domains is shown in **Figure 1B**.

Vif has been shown to self-associate both in vitro[33,41,59] and in vivo.[18,34] We thus focused our analysis on the characterization of Vif domains regarding their capacity to self-assemble, their secondary structure, together with their RNA binding and chaperone activities.

Biophysical analyses of HIV-1 Vif domains (NTD and CTD)

In a first set of experiments, samples of full-length Vif and of its truncated versions were used to analyze (1) their homogeneity by dynamic light scattering (DLS), (2) their secondary structure by circular dichroïsm (CD), and (3) their amenability to structural studies by NMR.

DLS was essential to assess the quality of protein samples before further experiments. We found that distributions of all Vif proteins appeared unimodal, and thus we could exclude disordered aggregation in our protein samples. The estimated polydispersity degree, which is indicative of the oligomerization modes of the protein, was between 30 to 40% (**Fig. 1C**). A mean hydrodynamic radius of 7.5 nm was measured for Vif in good agreement with previous studies.[46,47,49] For Vif domains, the hydrodynamic radii were slightly lower, varying from 4 to 5 nm (**Fig. 1C**), suggesting that Vif (1–150) and Vif (1–97) may also form multimers despite the absence of the ^{161}PPLP^{164} oligomerization motif. This is not surprising as domains outside this motif have been shown to contribute to multimerization.[34,47] Moreover, the ^{161}PPLP^{164} domain is not conserved among HIV-2 and SIV,[17] confirming that other unknown domains may be involved in oligomerization.

The secondary structure of Vif and its domains were further investigated using far-UV CD (**Table 1**). CD spectra in the far-UV domain (180–260 nm) give information on the secondary structure of proteins, namely their content in α-helix, β-strands, and random secondary structures. In good agreement with previous studies,[46,47,49] wild-type Vif is composed of 15% of α-helix,

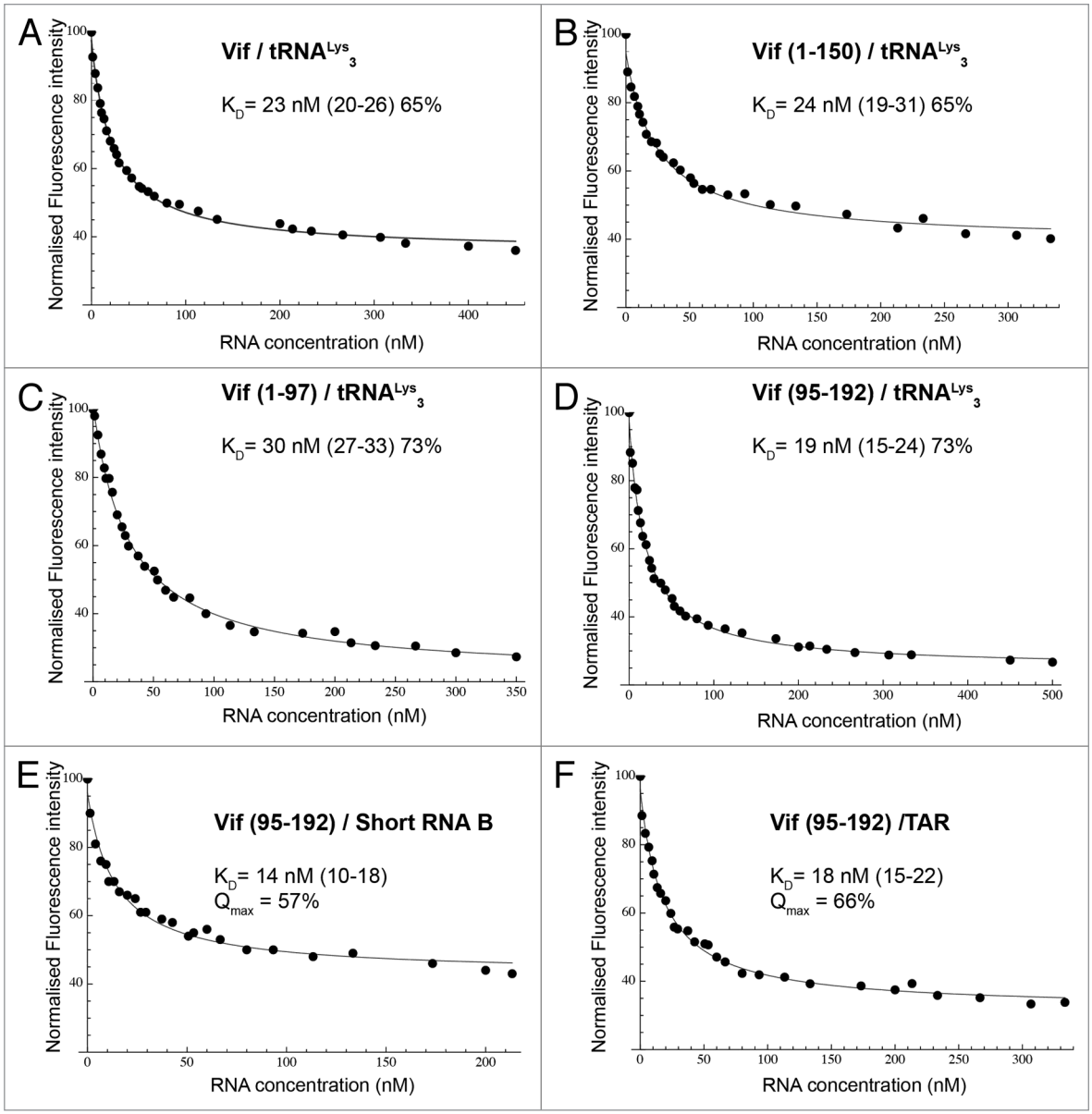

Figure 2. Fluorescence titrations of Vif and its domains with RNA at 25 °C. (**A**) Vif/tRNA$^{Lys}_3$, (**B**) Vif (1–150)/ tRNA$^{Lys}_3$, (**C**) Vif (1–97)/ tRNA$^{Lys}_3$, (**D**) Vif (95–192) tRNA$^{Lys}_3$, (**E**) Vif (95–192)/short RNAB and (**F**) Vif (95–192)/TAR. The dissociation constants (K_D) are indicated in nM with the 95% confidence interval between parentheses. The maximal fluorescence quenching (Q_{max}) obtained for each titration is indicated as a percentage (%). The measurements were performed in a TRIS-HCl (30 mM, pH 7.5) buffer containing 200 mM NaCl and 10 mM $MgCl_2$.

33% of β-strands and 52% of disordered regions. As expected from secondary structure prediction,[17] Vif (1–150) and Vif (1–97) show an overall structured organization, while Vif (95–192) is much less structured with only 35% of secondary structures (α-helix + β-strands). The sum of secondary structures predicted and observed by CD are very similar (**Table 1**), even if differences exist in the repartition of the secondary structures. It is possible that due to the great diversity of topologies found within proteins, the limited representation of secondary structural components within the CD reference databases provides a less accurate determination.[60] However, altogether our data point out that the percentage of random structures is smaller for Vif (1–150) and Vif (1–97), where the CTD is missing. Vif (1–97) presents the highest percentage of secondary structures (68%). This domain could have been amenable to structural study by NMR or X-ray crystallography. Unfortunately, its poor solubility prevented us from solving its 3D structure. We thus observed that the CTD of Vif is disordered in solution, while the NTD is the most structured region. Accordingly to the high percentage of random regions, the CD signal in the near-UV region, which is potentially informative about proteins tertiary structure, was nearly zero for all proteins tested.

We then studied the 1D ^{1}H NMR spectrum of Vif and its domains (**Fig. S1**). Taking into account that Vif forms multimers in solution, the poor dispersion of NMR signals in the amide region (7.5–10 ppm) indicated that the observable protons are not

involved in the hydrophobic core of the proteins, but belong to a less folded domain. This feature is confirmed by the observation that the 1D ^{1}H NMR spectrum of Vif and Vif (95–192) are identical. Therefore, the only observable part of the Vif protein by NMR is its CTD. We subsequently labeled Vif (95–192) by ^{15}N-nitrogen to analyze this domain by 2D NMR spectroscopy (**Fig. 1D**). Amide group signals were poorly dispersed in the proton dimension (0.5 ppm) and covered 10 ppm in the nitrogen dimension. The signal at 10.07 ppm corresponds to the indol NH of the unique tryptophan (W174) present in Vif (95–192). This proton signal is also observable in Vif spectrum while the other six tryptophan (W5, W11, W21, W38, W70, W79) indol protons remained unobservable. The poor dispersion of the amide groups and the linewidth of the NMR signals of Vif (95–192) confirmed that this protein is not structured and forms multimers. The addition of zinc ions did not allow further structuration, but an additional broadening of signals was observed. Regarding Vif (1–97), very few large signals are observed, indicating that this protein forms high molecular weight complex with a low percentage of unstructured regions.

Altogether, these biophysical analyses show that Vif NTD is highly structured, while the CTD is globally unfolded. These results reinforce the data in the literature suggesting that no interaction is expected between the N- and the C-terminal domains of Vif.[41,42,45]

The N- and C-terminal domains of HIV-1 Vif have both RNA binding capacity

According to rigorous analysis of binding parameters, it was previously shown that HIV-1 genomic RNA and A3G mRNA contain specific Vif binding sites.[12,46,47,49,50] Namely in the 5′-end of HIV-1 genomic RNA, Vif binds to the TAR, poly(A), SL1, and a short sequence within the Gag coding region (nucleotides 539–546).[50] In line with this study, we focused our attention on RNA B (500 nucleotide long RNA encompassing sequence 499–996 of HIV-1 genomic RNA) and on a shorter version of this RNA (sRNA B, nucleotides 499–800), which also contains a high affinity binding site for Vif.[46] We also investigated the interaction of Vif domains with the apical part of TAR (16 nts) corresponding to a minimal binding site for Vif (54), and to $tRNA^{Lys}_3$ (76 nts), which acts as a primer for HIV-1 reverse transcription. Indeed, Vif has previously been shown to promote the annealing of $tRNA^{Lys}_3$ to the PBS (Primer Binding Site), and also to inhibit in vitro the NCp7-mediated $tRNA^{Lys}_3$ annealing when both proteins are present.[52] As no data on the putative interaction between Vif and $tRNA^{Lys}_3$ are available, we investigated whether Vif is able to bind $tRNA^{Lys}_3$ by fluorescence and NMR spectroscopies. Actually, ^{15}N-labeled $tRNA^{Lys}_3$ and NMR assignment of its imino groups were already available in our group,[18,61] thereby allowing the use of NMR to study Vif binding to $tRNA^{Lys}_3$. To perform N^{15}-labeling, we used a recombinant $tRNA^{Lys}_3$ produced in *E. coli* and functional for the initiation of HIV-1 reverse transcription.[62] This recombinant tRNA does not bear all the post-transcriptional modifications carried by the human $tRNA^{Lys}_3$ but we assume that, as for NCp7,[63] post-transcriptional modifications are not a driving force for the interaction with Vif.

Table 2. Dissociation constants (K_D) derived from fluorescence titrations

	RNA B	sRNA B	$tRNA^{Lys}_3$	TAR
Vif				
K_D (nM) Q_{max}	30 ± 3 50%	13 ± 2 70%	27 ± 5 65%	31 ± 4 56%
Vif (1–97)				
K_D (nM) Q_{max}	31 ± 5 76%	10 ± 2 65%	34 ± 4 73%	32 ± 4 62%
Vif (95–192)				
K_D (nM) Q_{max}	26 ± 4 62%	16 ± 2 60%	16 ± 3 73%	20 ± 2 66%
Vif (1–150)				
K_D (nM) Q_{max}	47 ± 2 60%	27 ± 2 56%	51 ± 7 65%	31 ± 4 54%

Each K_D value is the average of five titrations, the mean standard deviation and the maximal attenuation Q_{max} are indicated.

To gain insights into interactions occurring between Vif protein domains and a panel of RNAs, we used fluorescence spectroscopy. Indeed, Vif contains 8 tryptophans that confer a high intrinsic fluorescence signal to the protein. Similarly, Vif (1–97) and Vif (1–150) have 7 tryptophan residues, while Vif (95–192) possesses only one. Because of their photophysical properties and their high sensitivity, tryptophans constitute a useful tool to determine binding parameters in protein-nucleic acids systems. Upon RNA binding, the fluorescence of Vif and its domains were attenuated (**Fig. 2**), and titration curves representing fluorescence quenching were appropriately fitted to determine dissociation constants (K_D). Titration curves of Vif proteins with $tRNA^{Lys}_3$ are presented in **Figure 2**, and the stoechiometry of the different structural domains of Vif in interaction with various RNAs is about one multimer per RNA (data not shown). **Table 2** summarized the obtained K_D values (see Materials and Methods). Dissociation constant analysis showed that Vif (1–97), which contains the RNA binding domain (residues 1–60), binds to all the RNAs tested with constants similar to full-length Vif (**Table 2**). Globally, the K_D magnitudes range from 10 to 34 nM, corresponding to a high binding affinity. We also showed that Vif (1–150) binds RNA less efficiently (**Table 2**), and corresponding K_D values range from 30 to 51 nM. This result indicates that the HCCH and SOCS-box domains do not participate to RNA binding, in agreement with previous results showing that no interaction could be observed between a peptide containing the HCCH motif and nucleic acids (J-C Paillart, unpublished data). More surprisingly, our data also show that Vif (95–192) strongly binds RNAs, with relative dissociation constants ranging from 16 to 26 nM (**Fig. 2**; **Table 2**). The K_D of Vif (95–192) for RNA is globally lower (or equal) than what observed in the case of Vif (1–97) for the same target (**Table 2**).

Our data also demonstrate for the first time that Vif, as NCp7, binds $tRNA^{Lys}_3$ with high affinity (K_D = 23 nM) and the corresponding dissociation constant is comparable to the one determined for NCp7 (K_D = 20 nM) at the same $MgCl_2$ concentration (**Table 2**).[63] The different domains of Vif also exhibited

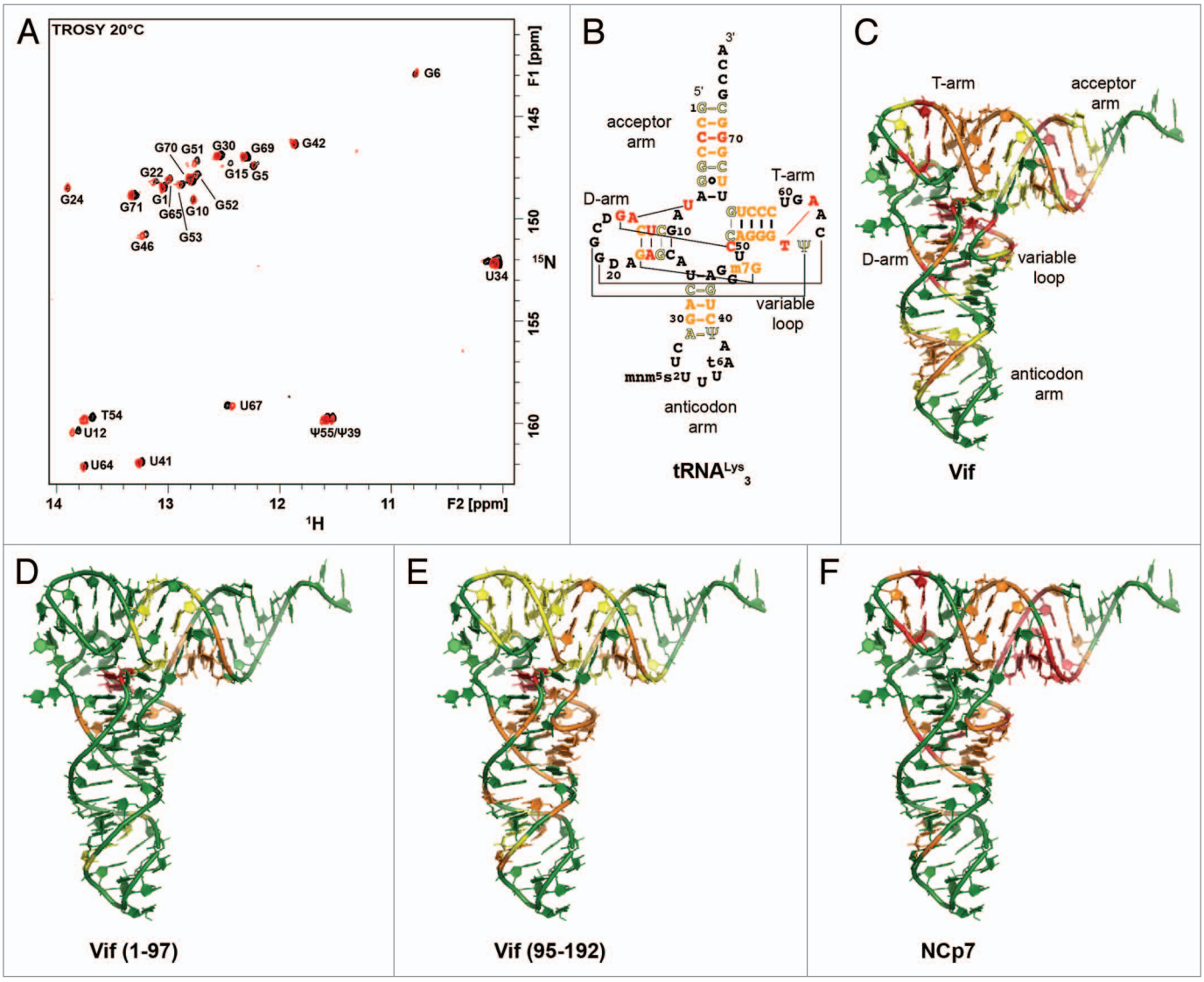

Figure 3. NMR chemical shift mapping of the binding sites of Vif proteins on $tRNA^{Lys}_3$. (**A**) Two NMR spectra (2D ^1H-^{15}N TROSY) acquired at 20 °C are superimposed: in black for $tRNA^{Lys}_3$ alone (reference spectrum) and in red for $tRNA^{Lys}_3$/Vif complex. (**B**) The NMR chemical shift mapping is reported on the secondary structure of $tRNA^{Lys}_3$ with the following color code: the base pairs for which the chemical shift variation of the imino group upon addition of the protein is ≥0.05 ppm are in red, between 0.03 and 0.05 ppm in orange and equal to 0.02 ppm in yellow. Mapping on the $tRNA^{Lys}_3$ 3D structure (PDB code 1FIR) of the binding sites of the Vif protein and its domains: (**C**) Vif, (**D**) Vif (1–97), (**E**) Vif (95–192) at 2 equivalents and (**F**) NCp7 at 3 equivalents.[64] The color code is the same as in B.

rather good affinity for small and highly structured RNAs such as TAR and $tRNA^{Lys}_3$ with very similar K_D values (**Table 2**). Interestingly, the comparison of K_D values obtained for RNA B and sRNA B leads to the observation that highly specific Vif binding sites are present in sRNA B (**Table 2**), confirming the presence of Vif preferential binding sites in this region of HIV-1 genomic RNA.[46] It is possible that these high affinity binding sites are somehow buried in the complete RNA B, while they are exposed in its shorter form and thus available to interact with Vif. Alternatively, in the case of RNA B, there could be additional non-specific interactions which contribute to increase the observed K_D value.

Our previous analysis on Vif interaction with various viral nucleic acids[46] showed that Vif specifically binds some DNA and RNA sequences. However, similarly to NCp7,[63] the highly basic character of Vif promotes its interaction with nucleic acids. Indeed, non-specific binding could be revealed through maximal fluorescence quenching (Q_{max}) values during titration. Globally, for non-specific binding, i.e., binding essentially driven by electrostatic interaction due to the highly basic character of Vif, Q_{max} ranges only from 20 to 40%. On the contrary, it reaches 60 to 70% for specific binding. Fluorescence titrations of Vif, Vif (1–97), and Vif (95–192) were also performed with a previously defined "non-specific RNA binder" of Vif, corresponding to a repetition of 10 cytosines (C10).[46] We thus showed that although Vif and its domains bind C10 with a dissociation constant around 40 nM, the relative Q_{max} values only reach 35%. We also tested the interaction of Vif with an *E. coli* tRNA extract. Noticeably,

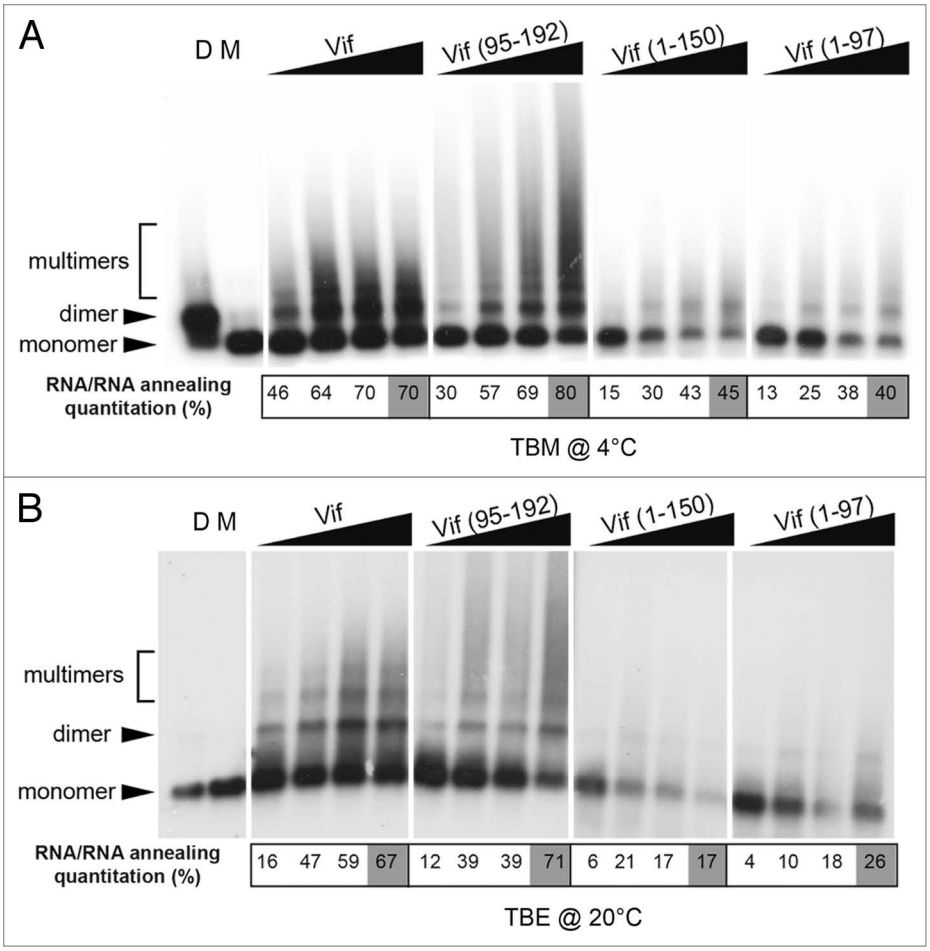

Figure 4. HIV-1 RNA dimerization induced by Vif and its domains. HIV RNA 1–615 was allowed to dimerize in the presence of increasing concentration of Vif, Vif (95–192), Vif (1–150), and Vif (1–97) (0.25, 0.5, 0.75 and 1 μM), and run on a 0.8% agarose gel in native (**A**), or semi-denaturing (**B**) conditions after protein removal. Lanes D and M correspond to control incubation of RNA in dimeric (D) or monomeric (M) buffers (see Materials and Methods for composition). Monomeric RNA and RNA/RNA complexes (dimers and multimers) were visualized and quantified using a FLA 5000 (Fuji). Quantitation is indicated under each panel and corresponds to the percentage of RNA/RNA annealing complex (dimer+multimer/ dimer+multimer+monomer).

Q_{max} reaches 23% (65% for $tRNA^{Lys}_3$) with a dissociation constant 3-fold higher than the one observed for $tRNA^{Lys}_3$, suggesting that Vif proteins interaction with C10 and total tRNA extract is mainly driven by electrostatic non-specific interactions.

Vif and NCp7 proteins share the same binding sites on $tRNA^{Lys}_3$

Our fluorescence analyses showed that Vif and its domains bind TAR and $tRNA^{Lys}_3$, two RNAs suitable for NMR studies. All our attempts to obtain TAR/Vif or Vif domains complexes at concentrations required for recording NMR spectra (around 10–40 μmol/l) were unsuccessful mainly due to massive precipitation of the protein/RNA complexes, thus preventing any further NMR studies. Fortunately, the situation was more favorable to investigate the binding of Vif and its domains to $tRNA^{Lys}_3$ by NMR chemical shift mapping. This method consists of labeling one of the partners of a complex with nitrogen 15 ($tRNA^{Lys}_3$ in our case) and in monitoring the variation of chemical shifts upon binding with the non-labeled partner (Vif or its domains). Indeed, ^{15}N-labeled $tRNA^{Lys}_3$ was produced as previously described[62] and the chemical shifts of its imino groups were used to monitor its interaction with Vif (**Fig. 3A**). The imino groups involved in the protein-binding site experience the largest variations of chemical shifts. For instance, the imino groups of U8, U12, G15, T54, and G70 undergo the largest variation of chemical shift, between 0.05 and 0.08 ppm upon Vif binding (**Fig. S2**). Our NMR data indicate that Vif is most strongly bound to the T-arm, the acceptor arm, the variable loop, and the D-arm of $tRNA^{Lys}_3$ (**Fig. 3B**). The NMR footprint more clearly appears when reported on the 3D structure of $tRNA^{Lys}_3$ (**Fig. 3C**). Thus, Vif presented a strong binding site located in the core of $tRNA^{Lys}_3$. Interestingly, Vif (1–97) (**Fig. 3D**) binds in the core of $tRNA^{Lys}_3$ at the junction between the T, acceptor and D arms. Vif (95–192) showed a more dispersed interaction but was still able to bind $tRNA^{Lys}_3$ T- and D-arms (**Fig. 3E**). Unfortunately, we were not able to examine Vif (1–150) binding to $tRNA^{Lys}_3$ due to the poor solubility of this protein. Interestingly, the NMR chemical shift mapping of Vif bound to $tRNA^{Lys}_3$ was almost identical with that of the one determined for NCp7[64] (**Fig. 3F**), suggesting that these two proteins share the same binding sites on $tRNA^{Lys}_3$. Taken together, these results suggest that the interaction with the T-arm of $tRNA^{Lys}_3$ is dependent on the CTD of Vif while the interaction in the core of $tRNA^{Lys}_3$ at the junction of the accepetor, T and D arms occurs through its NTD.

The RNA chaperone activity of Vif is driven by its C-terminal domain

In order to identify the domain of Vif involved in RNA chaperone activity, we compared the capacity of full-length Vif and its domains (1) to modulate HIV-1 RNA dimerization (**Fig. 4**) and (2) to activate the annealing of two complementary oligodeoxynucleotides (TAR(+)/TAR(-) assay) in vitro (**Fig. 5**).

HIV-1 RNA dimerization assay

HIV-1 RNA can form two different types of dimers in vitro, termed loose and tight dimers depending on their thermal stability that are correlated with the process of viral maturation after particle budding (for a review see ref. 65). Using an RNA fragment encompassing the first 615 nucleotides of HIV-1 genomic RNA, RNA dimerization was analyzed under two different

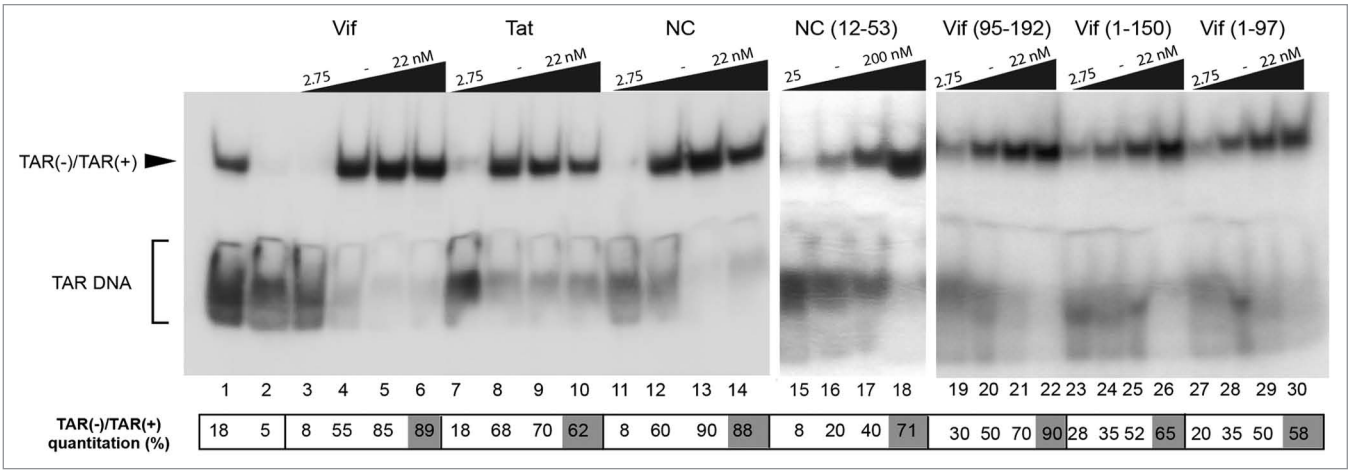

Figure 5. Stimulation of HIV-1 TAR(+)/TAR(-) DNA annealing by Vif and its domains. TAR(+) and ^{32}P-labeled TAR(-) DNA oligonucleotides were co-incubated in the presence of increasing concentrations of NCp7 (wild-type and fragment 12–53), Tat, and Vif (full-length and domains). The protein concentrations were 2.75, 5.50, 11, and 22 nM except for NC (12–53) for which the concentrations were 25, 50, 100 and 200 nM. In the absence of protein, double-stranded TAR DNA was formed upon incubation at 65 °C for 30 min (Ct+, lanes 1) but not at 37 °C (Ct-, lanes 2). TAR(+)/TAR(-) was annealed at 37 °C for 5 min with HIV-1 NCp7 (protein/nt molar ratios of 1/40, 1/20, 1/10 and 1/5) (lanes 11–14), Tat (lanes 7–10), Vif (lanes 3–6), NC (12–53) (lanes 15–18), Vif (95–192) (lanes 19–22), Vif (1–150) (lanes 23–26), and Vif (1–97) (lanes 27–30). TAR(+)/TAR(-) complexes were visualized and quantified using a FLA 5000 (Fuji). Quantitation is indicated under the panel and corresponds to the percentage of TAR(+)/TAR(-) DNA complexes (TAR(+)/TAR(-) / TAR(+)/TAR(-) + TAR DNA alone) after 5 min reaction.

electrophoresis conditions: (1) native conditions under which both loose and tight dimers are stable (**Fig. 4A**) and (2) semi-denaturing conditions in which only tight dimers are stable (**Fig. 4B**).[52] Vif and Vif (95–192), both stimulated RNA dimerization in a concentration dependent manner (**Fig. 4A**), with a dimerization yield of 70% and 80% at 1 μM Vif protein, respectively. This Vif-induced RNA dimer corresponds to tight dimer, as it is still observed under semi-denaturing conditions (**Fig. 4B**). Interestingly, these two Vif proteins were also able to induce the formation of multimers of RNAs, as previously observed[66,67] (**Fig. 4B**). However, while increasing concentration of Vif (1–150) and Vif (1–97) progressively increased the dimerization yield from 13–15 to 40–45% in native conditions (**Fig. 4A**), RNA dimers only marginally increased under semi-denaturing conditions (**Fig. 4B**). Surprisingly, a partial loss of RNA dimer signal was reproducibly observed for Vif (1–150) and Vif (1–97) (**Fig. 4A and B**). This is likely due to a higher degree of RNA aggregation of these two truncated forms, as previously observed for Pr55^{Gag} protein.[68] These results suggest that Vif (1–97) and Vif (1–150) were mainly able to induce the formation of loose dimers. Thus, Vif and Vif (95–192) mimic the NCp7-induced RNA dimerization activity suggesting that the RNA chaperone activity of Vif is partially mediated by its CTD encompassing Cul5 and EloC/B binding motifs as well as the PPLP sequence, and that this CTD is important, at least in vitro, to avoid the aggregation of the proteins.

TAR(+)/TAR(–) annealing assay

The annealing of complementary TAR sequences is essential to achieve (–) strand strong-stop DNA transfer, and among the various standard RNA chaperoning assays, the annealing of a TAR oligodeoxynucleotide (TAR+) to its complementary sequence (TAR-) has been used in many occasions.[48,54] To identify and confirm the potential Vif domain(s) involved in RNA chaperone activity, we compared at a define time point the ability of Vif and its domains to promote the annealing of two complementary TAR DNA sequences with that of NCp7, NC (12–53) (peptide 12–53 of NCp7) and Tat, two other RNA chaperone proteins. In the absence of protein, TAR(+)/TAR(–) annealing occurred at 65 °C in high salt conditions in the positive control (**Fig. 5**, lanes 1). No TAR(+)/TAR(–) annealing was observed at 37 °C in the negative control (**Fig. 5**, lane 2). Incubation with NCp7 or Tat at 37 °C for 5 min favored TAR(+)/TAR(–) annealing with an observed DNA complex yield at the highest protein concentration of 88 and 62%, respectively (**Fig. 5**, lanes 7 to 14). Interestingly, in presence of Vif, TAR(+)/TAR(–) annealing was also observed with a complex yield (89%) very similar to the one observed for NCp7 (**Fig. 5**, lanes 3–6), suggesting that Vif was as efficient as NC in TAR(+)/TAR(–) annealing activity. As expected from previous studies,[48,54,69] the NC (12–53) peptide was found to be poorly active in TAR-annealing activity and other RNA chaperone assays. Indeed, 71% of TAR annealed complex was obtained at 200 nM NC (12–53) (**Fig. 5**, lanes 15–18), whereas 20 times less Vif protein was necessary to obtain this percentage after 5 min reaction (**Fig. 5**, lane 5). Surprisingly, when we analyzed the truncated domains of Vif, we showed that all of them were able to stimulate TAR(–)/TAR(+) annealing but at different level compared with Vif (**Fig. 5**, lanes 19–30). While Vif (1–150) and Vif (1–97) gave a maximum of 65 and 58% of annealed complex, respectively, at the highest Vif concentration, Vif (95–192) was able to anneal 90% of TAR DNA (**Fig. 5**, lanes 19–22), a percentage close to the one observed for wild-type Vif.

Taken together, these two assays indicate that Vif possesses nucleic acid chaperone activity that is driven in part, but not only, by its C-terminal unstructured domain.

Discussion

In this study, we investigated the RNA binding and chaperoning activities of HIV-1 Vif. First, by using CD and NMR spectroscopies, we showed that the NTD of Vif, encompassing residues 1–97, is the most structured domain in solution, whereas the CTD (95–192) remains mainly unfolded either alone or within the full-length Vif. Therefore, even if we cannot definitely exclude subtle differences in the secondary structure of these domains alone or within the full-length Vif, our analysis suggests that their secondary structure contents are similar in these two states. Second, we showed that the NTD of Vif binds with high affinity to RNAs that were previously described as Vif preferential binding sites, such as TAR at the 5′-end of the HIV-1 genomic RNA and *gag* coding region.[46,50] This is in agreement with a previous study showing that a peptide from amino acids 1 to 64 of HIV-1 Vif possesses a strong RNA binding activity.[26] Indeed, highly conserved hydrophobic residues such as W11, Y30, and Y40 are present in the N-terminus of Vif from several primate lentivirus strains, and their mutation significantly decreased the binding of Vif to RNAs.[26] Unexpectedly, we showed that the CTD of Vif is also able to bind these RNAs with high affinity. Notably, Vif proteins from several strains of HIV-1, HIV-2, and SIV are composed of heterogeneous sequences notably in their CTD, yet their unfolded characteristic is conserved and they can functionally complement each other.[70,71] Moreover, while the sequences of Vif from HIV-1, HIV-2, and SIV strains are highly divergent in the CTD, a high number of arginines and lysines in the CTD of Vif (10–17 according to the strain), and thus a conservation of a significant net positive charge is still encountered. Therefore, the overall basic and unfolded character of the CTD of Vif in primate lentiviruses is conserved. This feature probably contributes to the RNA binding and chaperoning activities of Vif as such intrinsically disordered domains are proposed to support chaperone activity.[72-74] Interestingly, we showed that the CTD of Vif facilitates nucleic acid annealing as demonstrated in our HIV-1 RNA dimerization and TAR(+)/TAR(–) annealing assays. At this point, comparing NCp7 and Vif seems very interesting. NCp7 is the most efficient RNA chaperone protein encountered in HIV,[53] and our results show that the annealing activity of Vif is as efficient as NCp7 and slightly better than the one determined for Tat. The N-terminal basic residues of NCp7 are responsible for some of the RNA chaperone activity, like annealing and aggregation of nucleic acids, whereas the zinc-fingers are responsible for the specific destabilization of nucleic acids.[53] The efficiency of the NCp7 NTD to promote annealing of complementary RNA is essentially electrostatic, due to charge complementarities between nucleic acid backbone and positively charged residues,[18,61] and is exemplified in our experiments when we compared the annealing activity of NCp7 and NC (12–53) lacking the N-terminal part (**Fig. 5**). Actually, NC (12–53) has lost most of its annealing activity (20 times less efficient than NCp7 and Vif). Interestingly, the basic and unfolded CTD of Vif clearly drives nucleic acids annealing activity of the protein, suggesting that the RNA chaperone activity of Vif and NCp7 is partially driven by their basic unfolded domains, at least regarding their annealing activities. More generally, many proteins do not have well-ordered structures in their functional parts, representing hybrids containing both ordered and disordered regions. Coherently, the highly structured Vif NTD is responsible for a specific interaction with nucleic acids, similarly to NCp7 that specifically binds RNA via its zinc-knuckles.[75] Contrary to what was observed with NCp7, whether zinc binding could enhance the RNA annealing activity of Vif is still a matter of debate. First, it has been shown in vitro that full-length Vif and short Vif peptides corresponding to the HCCH motif (amino acids 101–142) are capable to bind zinc with high specificity but zinc binding induces conformational change that leads to the formation of large aggregates.[76] Second, a peptide containing the HCCH motif is not able to bind nucleic acids, independently on the presence of zinc (JC Paillart, unpublished data), suggesting that the HCCH and SOCS-box domains do not participate to RNA binding. Altogether, it seems that the NTD of Vif specifically binds Vif cognate RNAs, whereas the CTD possesses the ability to bind RNAs with a strong RNA annealing activity. Moreover, in good agreement with previous in vitro analyses,[12,46,47,50] these data suggest that the C-terminal His-tag used to purify Vif did not have a significant impact on the functional properties of Vif structural domains.

For the first time, we showed, that Vif can directly bind $tRNA^{Lys}_3$, the primer of HIV-1 reverse transcription. Indeed, the NTD has a definite and specific binding site to the inside of the L-shape of $tRNA^{Lys}_3$, whereas the fingerprint with the CTD is more diffused, most likely indicating a less specific binding. Moreover, the CTD is responsible for the interaction with the T-arm of $tRNA^{Lys}_3$, whereas the NTD of Vif is not able to bind this arm that needs to be annealed to the PBS to promote efficient initiation of reverse transcription. Interestingly, NMR chemical shift mapping demonstrates that Vif and NCp7 share the same binding sites on $tRNA^{Lys}_3$. We previously showed in vitro that Vif promotes hybridization between viral RNA and $tRNA^{Lys}_3$ generating a functional complex, but that the initial steps of reverse transcription (addition of the first nucleotides) are inhibited by Vif.[52] In presence of NCp7, Vif was shown to inhibit NCp7-assisted hybridization of $tRNA^{Lys}_3$ to viral RNA.[52] Our results are not surprising regarding the fact that Vif and NCp7 share the same binding site on $tRNA^{Lys}_3$ (**Fig. 3**), thus leading to the conclusion that Vif and NCp7 are probably in competition for the same binding sites therefore inhibiting premature reverse transcription[77,78] during the early steps of viral assembly. It is more likely that the inhibiting effect of Vif would be reduced during and/or after virion assembly since less than 100 Vif are packaged into viral particles.[13,79,80] After this step, $Pr55^{Gag}$ is processed by viral protease to give matured NCp7 whose concentration exceeds rapidly that of Vif, thus preventing Vif inhibition on reverse transcription.

In summary, we showed that HIV-1 Vif is a complex RNA binding protein involving both its structured NTD, through conserved hydrophobic residues, and its unfolded CTD through non-specific electrostatic interactions. Interestingly, this latter domain seems responsible for most of the RNA chaperone activity of Vif, and this feature is strongly correlated with the unfolded nature of the CTD. Although we observed that Vif and NCp7 interact with common $tRNA^{Lys}_3$ motifs, their exact role during the initial steps of reverse transcription will need further investigation.

Materials and Methods

Expression and purification of Vif and its domains

Vif expression vectors were constructed by PCR and cloning into the pET-52b(+) vector (Novagen). First, pD10Vif expression vector (Vif HXB2) was PCR-amplified with the corresponding forward (F) and reverse (R) primers: (F Vif) 5′GGTCCATGG AAAACAGATG GCAG3′ and (R Vif) 5′GGTGAGCTCG TGTCCATTCA TTGTG3′; (R Vif 1–97) 5′GGTGAGCTCT TGTGTGCTAT ATCTCTT3′; (R Vif1–150) 5′GGTGAGCTCT AGTGCCAAGT ATTGTAG3′ giving rise to vectors expressing full-length Vif, domains 1–97 and 1–150 of Vif, respectively. Primers (F Vif95–192) 5′GGTCCATGG TAGACCCTGA ACTAGCAGAC3′ and (R Vif 95–192) 5′CACAATGAAT GGACACGAGC TC3′ were used to generate a plasmid expressing domain 95–192 of Vif. Forward primers contain a NcoI restriction site (underlined) while reverse primers contain a SacI restriction site (underlined). After purification of the PCR products (Nucleospin PCR clean-up, Macherey Nagel), DNA fragments were digested with NcoI and SacI, and cloned into pET-52b(+) vector previously digested with the same restriction enzymes. The sequence of all constructs, pET52b(+) Vif, Vif (1–97), Vif (1–150) and Vif (95–192), was confirmed by DNA sequencing (GATC Biotech).

Escherichia coli BL21(DE3) competent cells were transformed with plasmids coding for Vif, Vif (1–97), Vif (1–150), and Vif (95–192). Expression of Vif and its domains were induced by addition of 1 mM IPTG in exponential phase of cultures (absorbance at 600 nm around 0.6). After 3 h of induction at 37 °C, bacteria were harvested by centrifugation at 6000 g during 15 min, lysed in denaturing lysis buffer (6 M guanidine hydrochloride, 100 mM sodium phosphate, 10 mM TRIS-HCl pH 8) at room temperature and stirred overnight. Cellular debris was separated by centrifugation at 27 000 g during 30 min at 4 °C and the cleared lysate was loaded onto a Ni-NTA agarose column. The column was washed with lysis buffer and elution was performed by decreasing the pH from 6.5 to 4.5. Fractions containing Vif proteins were analyzed on 14% SDS–PAGE and pooled. Proteins were then renatured by slow dialysis against buffers with decreasing guadinium chloride concentration, and finally against the following buffers: Vif (50 mM MOPS, 1 mM DTT, 50 mM NaCl, pH 6.5), Vif (1–97) (50 mM MOPS, 50 mM NaCl pH 6.5), Vif (95–192) (50 mM MES pH 6.5, 9.6 mM NaCl, 0.4 mM KCl, 2 mM $MgCl_2$, 2 mM $CaCl_2$, 1 mM DTT), and Vif (1–150) (50 mM MOPS pH 6.5, 1 mM DTT, 50 mM NaCl). The same protocol was followed to produce ^{15}N-labeled Vif (95–192) except that the LB media was changed for spectra 9 (^{15}N) media (Cambridge isotope laboratories or Cortecnet). The proteins were concentrated using Centriprep YM 3 (Millipore) up to 0.4 mg/mL and ultracentrifuged at 100 000 g for 30 min at 4 °C before adding 10% glycerol. Vif proteins were then stored at 4 °C and immediately prior to use Vif, stock solutions were ultracentrifuged at 100 000 g for 30 min at 4 °C to eliminate aggregates in solution. For NMR studies, no glycerol was added.

Nucleic acids preparation

Plasmids pHXB2 corresponding to parts of *gag* were obtained as previously described.[50] To express RNA fragments corresponding to nucleotides 499–996 (RNA B) and 499–799 (Short RNA B) of HIV-1 genome, plasmids were linearized with PvuII and SalI, respectively, and then used as template for in vitro run off transcription with bacteriophage T7 RNA polymerase under conditions previously described.[81] After 3 h at 37 °C, the reaction mixture was incubated for 1 h at 37 °C with RNase-free DNase I (Roche), and then extracted with phenol-chloroform. RNAs were then purified with FPLC (Pharmacia) using a TSK250/G2000SW column (TOSOH Bioscience) in a buffer containing 200 mM sodium acetate (pH 6.5) and 1% (v/v) methanol as previously described,[66] precipitated in ethanol and dissolved in Milli-Q water (Millipore) prior to use.

^{15}N-labeled $tRNA^{Lys}_3$ was expressed in *E. coli* (JM101TR strain) from a recombinant plasmid and purified as previously described.[62] The RNA oligonucleotide corresponding to the apical part of the TAR hairpin ($^{5'}$CGAGCCUGGG AGCUCG$^{3'}$) was purchased from Microsynth or Dharmacon and purified using HPLC (ÄKTA design-Unicorn) system with a (PA-100) anion exchange column (Dionex), and concentrated with Centricon ® (Millipore).

Dynamic light scattering (DLS)

Samples were prepared in their buffers, and final protein sample concentrations were determined after ultracentrifugation. Intensities of scattered light and correlation times were measured with a Zetasizer Nano S (Malvern). Measurements were performed in a single 50 µl trUView cuvette (Biorad Laboratories), maintained at 20 °C. DLS fluctuations of the scattering intensity due to Brownian motion were recorded at microsecond time intervals. An autocorrelation function was then derived, allowing determination of diffusion coefficients, D. Assimilating proteins in solution to spheres, diffusion coefficients were related to the hydrodynamic radius of the particles (R_h) via the Stokes-Einstein equation:

$$D = kT / R_h 6\pi \mu$$

in which k is the Boltzmann constant, T the temperature (K), and µ the solvent viscosity. All experimental data were corrected for solvent viscosity (measured with a 3.5 ml micro-Ubbelohde capillary viscosimeter tube from Schott), and refractive index (measured with an Abbe's refractometer). To analyze the oligomerization state of Vif and its functional domains, scattering data were then analyzed using DLS analysis software (Malvern).

Circular dichroism (CD)

Vif protein samples were prepared anaerobically in 50 mM MOPS, 150 mM NaCl, pH 6.5. Far-UV CD spectra (190–250 nm) were measured with a Jasco J-810 spectropolarimeter (Jasco Inc.). Samples were placed in rectangular quartz cuvettes of 2 mm path length maintained at 20 °C. Spectra were acquired at 50 nm/min with a time constant of 1 s and bandwidth equal to 1 nm. Each spectrum represents the average of at least 15 successive baseline-corrected scans. The mean residue molar ellipticity was determined according to equation: $[\theta] = (\theta \bullet M_R)/(10 \bullet \lambda \bullet c)$

where θ is the measured ellipticity in millidegrees, M_R is the mean residue mass, λ the optical path length and c, the protein concentration. Deconvolution of far-UV CD spectra and consequent secondary structure of protein content was estimated by Dichroweb (http://dichroweb.cryst.bbk.ac.uk/html/home.shtml).

Steady-state fluorescence measurements

Fluorescence measurements were recorded in quartz cells at 20 ± 0.2 °C on a Fluoromax-4 fluorometer (HORIBA Jobin-Yvon Inc.). The excitation wavelength was set at 295 nm for selective excitation of Trp residues. The emission wavelength was scanned from 310 to 500 nm. The integration time was 0.1 s, and the excitation and emission bandwidths were 5 nm. Fluorescence titrations were performed by adding increasing amounts of nucleic acid to 100 nM of protein in 30 mM Tris–HCl (pH 7.5), 200 mM NaCl, and 10 mM $MgCl_2$. Fluorescence intensities were then corrected for buffer fluorescence and dilution effect. To determine the binding parameters of Vif proteins to RNA fragments, we measured the decrease of the fluorescence intensity, I, at a fixed concentration of protein in presence of increasing RNA concentrations. Fluorescence intensities were corrected for dilution and were fitted using the following equation:

$$I = I_0 - \frac{I_0 - I_\infty}{2nN_t}\left(K_d + L_t + nN_t - \sqrt{K_d + L_t + nN_t}^{2} - 4L_t nN_t\right)$$

where I_0: Fluorescence intensity of protein without RNA; I: fluorescence intensity at a given concentration of RNA; I_∞: fluorescence intensity at the plateau of binding titration; n: number of RNA binding sites on the protein; L_t: total concentration of RNA; N_t: total concentration of protein. Confidence limits on the K_D were estimated by Monte-Carlo sampling using the MC-Fit program.[82]

NMR chemical shift mapping

NMR data were recorded at 20 °C on a Bruker Avance DRX600 spectrometer equipped with a TCI cryoprobe. 1D ^1H NMR spectra were recorded using a watergate sequence for solvent suppression.[83] 512 scans were usually acquired. ^1H-^{15}N TROSY experiments[84] were performed with 128 t1 increments and 2048 t2 data points per increment. The t1 dimension was acquired with the echo-antiecho method. For Vif (1–97) at 40 μM and Vif (95–192) at 36 μM, 1 equivalent of $tRNA^{Lys}_3$ stock at 0.9 mM was directly added to the protein sample. For full-length Vif, the previous operating mix led to precipitation of the protein. So, the complex components were mixed diluted at a 1:1 ratio and were then concentrated in a Centriprep YM 3 (Millipore) to a final concentration of each species around 20 μM.

Chemical shift variations Δ(H,N) were derived from ^1H and ^{15}N shift differences: $\Delta(H,N) = [(\Delta^{15}N\ W_N)^2 + (\Delta^1H\ W_H)^2]^{1/2}$, where $\Delta = \delta_{complex} - \delta_{free}$ ($\delta_{complex}$ is the chemical shift of the imino group in the complex and δ_{free} is the chemical shift of the imino group when $tRNA^{Lys}_3$ is free in solution), $W_H = 1$ for the proton chemical shift variation and $W_N = 1/6$ for the nitrogen chemical shift variation.

RNA chaperone activity

DNA and RNA substrates

Oligodeoxynucleotides (ODNs) used for the TAR(+)/TAR(–) DNA annealing assay corresponded to nucleotides 1–56 of the HIV-1 RNA sequence (MAL isolate, Accession Number X04415.1) in the sense and antisense orientations, as previously described.[48] TAR(+): 5′-GGTCTCTCTT GTTAGACCAG GTCGAGCCCG GGAGCTCTCT GGCTAGCAAG GAACCC-3′ and TAR(-): 5′-GGGTTCCTTG CTAGCCAGAG AGCTCCCGGG CTCGACCTGG TCTAACAAGA GAGAC-3′. RNA fragments used in the RNA dimerization assay corresponded to nts 1–615 of the HIV-1 MAL genomic RNA.

Proteins

HIV-1 NCp7 and NC (12–53) proteins were synthesized and purified as described.[85] The HIV-1 Tat protein was synthesized as reported in ref. 48.

RNA dimerization assay

RNA dimerization was performed as described previously.[52] Briefly, 100 nM of unlabeled HIV-1 1–615 RNA fragment were diluted in 10 μl of water together with the corresponding labeled RNA (5,000 cpm, 3–5 nM). Samples were denatured for 2 min at 90 °C, and snap-cooled on ice for 2 min. Dimerization was initiated by addition of Vif proteins under conditions disfavoring salt-induced RNA dimerization, or so called monomeric buffer (50 mM sodium cacodylate pH 7.5, 50 mM NaCl, 0.1 mM $MgCl_2$). When no protein was used to induce RNA dimerization, high salt dimeric buffer was used (50 mM sodium cacodylate pH 7.5, 300 mM NaCl, 5 mM $MgCl_2$). RNA samples were incubated 30 min at 37 °C, deproteinized, and resuspended in glycerol-containing loading buffer, split in two equal volumes and analyzed on a 0.8% agarose gel in native (Tris–Borate 0.5X, $MgCl_2$ 0.1 mM, run at 4 °C) or semi-denaturing (TBE 1X, run at 20 °C) electrophoresis conditions. Gels were fixed in 10% trichloroacetic acid for 10 min and dried for 1 h under vacuum at room temperature. Radioactive bands corresponding to monomeric and dimeric species were visualized and quantified using a FLA 5000 (Fuji).

TAR(–)/TAR(+) DNA annealing assay

The DNA annealing assay was performed as described in.[18,48] Briefly, 0.03 pmol of the TAR(+) and ^{32}P-TAR(–) ODNs were incubated in 10 μl of buffer A (20 mM TRIS-HCl pH 7.0, 30 mM NaCl, 0.1 mM $MgCl_2$, 5 mM DTT, and 10 μM $ZnCl_2$) with increasing concentrations of Vif, NCp7 or Tat proteins, as indicated in legend of **Figure 5**. Reactions were performed at 37 °C for 5 min except for the positive control that was incubated at 65 °C. To stop the reaction and remove the protein from the ^{32}P-ODN, 5 μl of a solution containing 20% glycerol, 20 mM EDTA pH 8.0, 2% SDS, 0.25% bromophenol blue, and 0.4 mg/

ml calf liver tRNA were added. Samples were resolved by 8% native PAGE in 50 mM Tris–borate pH 8.3, 1 mM EDTA at 4 °C. Subsequently, gels were fixed, autoradiographed, and the amounts of labeled single-stranded and double-stranded DNA were visualized and quantified using a FLA 5000 (Fuji).

Disclosure of Potential Conflicts of Interest

No potential conflicts of interest were disclosed.

Acknowledgments

We are grateful to Drs. Roland Marquet and Redmond Smyth for critical reading of the manuscript. We thank Dr. Jean-Luc Darlix (UMR 7213 CNRS, Université de Strasbourg) for the gift of TAR(+)/TAR(–) system. This work was supported by grants from the French National Agency for Research on AIDS and Viral Hepatitis (ANRS) to C.T., J.C.P. and S.B., and by doctoral fellowships from ANRS to S.X.G.

Supplemental Materials

Supplemental materials may be found here: www.landesbioscience.com/journals/rnabiology/article/29546/

References

1. Harris RS, Hultquist JF, Evans DT. The restriction factors of human immunodeficiency virus. J Biol Chem 2012; 287:40875-83; PMID:23043100; http://dx.doi.org/10.1074/jbc.R112.416925
2. Sheehy AM, Gaddis NC, Choi JD, Malim MH. Isolation of a human gene that inhibits HIV-1 infection and is suppressed by the viral Vif protein. Nature 2002; 418:646-50; PMID:12167863; http://dx.doi.org/10.1038/nature00939
3. Mangeat B, Turelli P, Caron G, Friedli M, Perrin L, Trono D. Broad antiretroviral defence by human APOBEC3G through lethal editing of nascent reverse transcripts. Nature 2003; 424:99-103; PMID:12808466; http://dx.doi.org/10.1038/nature01709
4. Mariani R, Chen D, Schröfelbauer B, Navarro F, König R, Bollman B, Münk C, Nymark-McMahon H, Landau NR. Species-specific exclusion of APOBEC3G from HIV-1 virions by Vif. Cell 2003; 114:21-31; PMID:12859895; http://dx.doi.org/10.1016/S0092-8674(03)00515-4
5. Bishop KN, Holmes RK, Malim MH. Antiviral potency of APOBEC proteins does not correlate with cytidine deamination. J Virol 2006; 80:8450-8; PMID:16912295; http://dx.doi.org/10.1128/JVI.00839-06
6. Marin M, Rose KM, Kozak SL, Kabat D. HIV-1 Vif protein binds the editing enzyme APOBEC3G and induces its degradation. Nat Med 2003; 9:1398-403; PMID:14528301; http://dx.doi.org/10.1038/nm946
7. Mehle A, Goncalves J, Santa-Marta M, McPike M, Gabuzda D. Phosphorylation of a novel SOCS-box regulates assembly of the HIV-1 Vif-Cul5 complex that promotes APOBEC3G degradation. Genes Dev 2004; 18:2861-6; PMID:15574592; http://dx.doi.org/10.1101/gad.1249904
8. Yu X, Yu Y, Liu B, Luo K, Kong W, Mao P, Yu XF. Induction of APOBEC3G ubiquitination and degradation by an HIV-1 Vif-Cul5-SCF complex. Science 2003; 302:1056-60; PMID:14564014; http://dx.doi.org/10.1126/science.1089591
9. Jäger S, Kim DY, Hultquist JF, Shindo K, LaRue RS, Kwon E, Li M, Anderson BD, Yen L, Stanley D, et al. Vif hijacks CBF-β to degrade APOBEC3G and promote HIV-1 infection. Nature 2012; 481:371-5; PMID:22190037
10. Zhang W, Du J, Evans SL, Yu Y, Yu XF. T-cell differentiation factor CBF-β regulates HIV-1 Vif-mediated evasion of host restriction. Nature 2012; 481:376-9; PMID:22190036
11. Hultquist JF, Binka M, LaRue RS, Simon V, Harris RS. Vif proteins of human and simian immunodeficiency viruses require cellular CBFβ to degrade APOBEC3 restriction factors. J Virol 2012; 86:2874-7; PMID:22205746
12. Mercenne G, Bernacchi S, Richer D, Bec G, Henriet S, Paillart JC, Marquet R. HIV-1 Vif binds to APOBEC3G mRNA and inhibits its translation. Nucleic Acids Res 2010; 38:633-46; PMID:19910370; http://dx.doi.org/10.1093/nar/gkp1009
13. Kao S, Khan MA, Miyagi E, Plishka R, Buckler-White A, Strebel K. The human immunodeficiency virus type 1 Vif protein reduces intracellular expression and inhibits packaging of APOBEC3G (CEM15), a cellular inhibitor of virus infectivity. J Virol 2003; 77:11398-407; PMID:14557625; http://dx.doi.org/10.1128/JVI.77.21.11398-11407.2003
14. Stopak K, de Noronha C, Yonemoto W, Greene WC. HIV-1 Vif blocks the antiviral activity of APOBEC3G by impairing both its translation and intracellular stability. Mol Cell 2003; 12:591-601; PMID:14527406; http://dx.doi.org/10.1016/S1097-2765(03)00353-8
15. Opi S, Kao S, Goila-Gaur R, Khan MA, Miyagi E, Takeuchi H, Strebel K. Human immunodeficiency virus type 1 Vif inhibits packaging and antiviral activity of a degradation-resistant APOBEC3G variant. J Virol 2007; 81:8236-46; PMID:17522211; http://dx.doi.org/10.1128/JVI.02694-06
16. Goila-Gaur R, Strebel K. HIV-1 Vif, APOBEC, and intrinsic immunity. Retrovirology 2008; 5:51; PMID:18577210; http://dx.doi.org/10.1186/1742-4690-5-51
17. Barraud P, Paillart JC, Marquet R, Tisné C. Advances in the structural understanding of Vif proteins. Curr HIV Res 2008; 6:91-9; PMID:18336256; http://dx.doi.org/10.2174/157016208783885056
18. Batisse J, Guerrero S, Bernacchi S, Sleiman D, Gabus C, Darlix JL, Marquet R, Tisné C, Paillart JC. The role of Vif oligomerization and RNA chaperone activity in HIV-1 replication. Virus Res 2012; 169:361-76; PMID:22728817; http://dx.doi.org/10.1016/j.virusres.2012.06.018
19. Dang Y, Wang X, York IA, Zheng YH. Identification of a critical T(Q/D/E)x5ADx2(I/L) motif from primate lentivirus Vif proteins that regulate APOBEC3G and APOBEC3F neutralizing activity. J Virol 2010; 84:8561-70; PMID:20592083; http://dx.doi.org/10.1128/JVI.00960-10
20. Russell RA, Pathak VK. Identification of two distinct human immunodeficiency virus type 1 Vif determinants critical for interactions with human APOBEC3G and APOBEC3F. J Virol 2007; 81:8201-10; PMID:17522216; http://dx.doi.org/10.1128/JVI.00395-07
21. Schröfelbauer B, Senger T, Manning G, Landau NR. Mutational alteration of human immunodeficiency virus type 1 Vif allows for functional interaction with nonhuman primate APOBEC3G. J Virol 2006; 80:5984-91; PMID:16731937; http://dx.doi.org/10.1128/JVI.00388-06
22. Tian C, Yu X, Zhang W, Wang T, Xu R, Yu XF. Differential requirement for conserved tryptophans in human immunodeficiency virus type 1 Vif for the selective suppression of APOBEC3G and APOBEC3F. J Virol 2006; 80:3112-5; PMID:16501124; http://dx.doi.org/10.1128/JVI.80.6.3112-3115.2006
23. Zhang W, Chen G, Niewiadomska AM, Xu R, Yu XF. Distinct determinants in HIV-1 Vif and human APOBEC3 proteins are required for the suppression of diverse host anti-viral proteins. PLoS One 2008; 3:e3963; PMID:19088851; http://dx.doi.org/10.1371/journal.pone.0003963
24. Pery E, Rajendran KS, Brazier AJ, Gabuzda D. Regulation of APOBEC3 proteins by a novel YXXL motif in human immunodeficiency virus type 1 Vif and simian immunodeficiency virus SIVagm Vif. J Virol 2009; 83:2374-81; PMID:19109396; http://dx.doi.org/10.1128/JVI.01898-08
25. Binka M, Ooms M, Steward M, Simon V. The activity spectrum of Vif from multiple HIV-1 subtypes against APOBEC3G, APOBEC3F, and APOBEC3H. J Virol 2012; 86:49-59; PMID:22013041; http://dx.doi.org/10.1128/JVI.06082-11
26. Zhang H, Pomerantz RJ, Dornadula G, Sun Y. Human immunodeficiency virus type 1 Vif protein is an integral component of an mRNP complex of viral RNA and could be involved in the viral RNA folding and packaging process. J Virol 2000; 74:8252-61; PMID:10954522; http://dx.doi.org/10.1128/JVI.74.18.8252-8261.2000
27. Khan MA, Aberham C, Kao S, Akari H, Gorelick R, Bour S, Strebel K. Human immunodeficiency virus type 1 Vif protein is packaged into the nucleoprotein complex through an interaction with viral genomic RNA. J Virol 2001; 75:7252-65; PMID:11461998; http://dx.doi.org/10.1128/JVI.75.16.7252-7265.2001
28. Hultquist JF, Binka M, LaRue RS, Simon V, Harris RS. Vif proteins of human and simian immunodeficiency viruses require cellular CBFβ to degrade APOBEC3 restriction factors. J Virol 2012; 86:2874-7; PMID:22205746; http://dx.doi.org/10.1128/JVI.06950-11
29. Mehle A, Thomas ER, Rajendran KS, Gabuzda D. A zinc-binding region in Vif binds Cul5 and determines cullin selection. J Biol Chem 2006; 281:17259-65; PMID:16636053; http://dx.doi.org/10.1074/jbc.M602413200
30. Xiao Z, Ehrlich E, Luo K, Xiong Y, Yu XF. Zinc chelation inhibits HIV Vif activity and liberates antiviral function of the cytidine deaminase APOBEC3G. FASEB J 2007; 21:217-22; PMID:17135358; http://dx.doi.org/10.1096/fj.06-6773com
31. Yu Y, Xiao Z, Ehrlich ES, Yu X, Yu XF. Selective assembly of HIV-1 Vif-Cul5-ElonginB-ElonginC E3 ubiquitin ligase complex through a novel SOCS box and upstream cysteines. Genes Dev 2004; 18:2867-72; PMID:15574593; http://dx.doi.org/10.1101/gad.1250204

32. Stanley BJ, Ehrlich ES, Short L, Yu Y, Xiao Z, Yu XF, Xiong Y. Structural insight into the human immunodeficiency virus Vif SOCS box and its role in human E3 ubiquitin ligase assembly. J Virol 2008; 82:8656-63; PMID:18562529; http://dx.doi.org/10.1128/JVI.00767-08
33. Yang S, Sun Y, Zhang H. The multimerization of human immunodeficiency virus type I Vif protein: a requirement for Vif function in the viral life cycle. J Biol Chem 2001; 276:4889-93; PMID:11071884; http://dx.doi.org/10.1074/jbc.M004895200
34. Batisse J, Guerrero SX, Bernacchi S, Richert L, Godet J, Goldschmidt V, Mély Y, Marquet R, de Rocquigny H, Paillart JC. APOBEC3G impairs the multimerization of the HIV-1 Vif protein in living cells. J Virol 2013; 87:6492-506; PMID:23576497; http://dx.doi.org/10.1128/JVI.03494-12
35. Douaisi M, Dussart S, Courcoul M, Bessou G, Lerner EC, Decroly E, Vigne R. The tyrosine kinases Fyn and Hck favor the recruitment of tyrosine-phosphorylated APOBEC3G into vif-defective HIV-1 particles. Biochem Biophys Res Commun 2005; 329:917-24; PMID:15752743; http://dx.doi.org/10.1016/j.bbrc.2005.02.057
36. Bouyac M, Courcoul M, Bertoia G, Baudat Y, Gabuzda D, Blanc D, Chazal N, Boulanger P, Sire J, Vigne R, et al. Human immunodeficiency virus type 1 Vif protein binds to the Pr55Gag precursor. J Virol 1997; 71:9358-65; PMID:9371595
37. Simon JH, Carpenter EA, Fouchier RA, Malim MH. Vif and the p55(Gag) polyprotein of human immunodeficiency virus type 1 are present in colocalizing membrane-free cytoplasmic complexes. J Virol 1999; 73:2667-74; PMID:10074112
38. Goncalves J, Shi B, Yang X, Gabuzda D. Biological activity of human immunodeficiency virus type 1 Vif requires membrane targeting by C-terminal basic domains. J Virol 1995; 69:7196-204; PMID:7474141
39. Kataropoulou A, Bovolenta C, Belfiore A, Trabatti S, Garbelli A, Porcellini S, Lupo R, Maga G. Mutational analysis of the HIV-1 auxiliary protein Vif identifies independent domains important for the physical and functional interaction with HIV-1 reverse transcriptase. Nucleic Acids Res 2009; 37:3660-9; PMID:19369217; http://dx.doi.org/10.1093/nar/gkp226
40. Guo Y, Dong L, Qiu X, Wang Y, Zhang B, Liu H, Yu Y, Zang Y, Yang M, Huang Z. Structural basis for hijacking CBF-β and CUL5 E3 ligase complex by HIV-1 Vif. Nature 2014; 505:229-33; PMID:24402281; http://dx.doi.org/10.1038/nature12884
41. Auclair JR, Green KM, Shandilya S, Evans JE, Somasundaran M, Schiffer CA. Mass spectrometry analysis of HIV-1 Vif reveals an increase in ordered structure upon oligomerization in regions necessary for viral infectivity. Proteins 2007; 69:270-84; PMID:17598142; http://dx.doi.org/10.1002/prot.21471
42. Marcsisin SR, Narute PS, Emert-Sedlak LA, Kloczewiak M, Smithgall TE, Engen JR. On the solution conformation and dynamics of the HIV-1 viral infectivity factor. J Mol Biol 2011; 410:1008-22; PMID:21763503; http://dx.doi.org/10.1016/j.jmb.2011.04.053
43. Reingewertz TH, Benyamini H, Lebendiker M, Shalev DE, Friedler A. The C-terminal domain of the HIV-1 Vif protein is natively unfolded in its unbound state. Protein Eng Des Sel 2009; 22:281-7; PMID:19218568; http://dx.doi.org/10.1093/protein/gzp004
44. Reingewertz TH, Shalev DE, Friedler A. Structural disorder in the HIV-1 Vif protein and interaction-dependent gain of structure. Protein Pept Lett 2010; 17:988-98; PMID:20450485; http://dx.doi.org/10.2174/092986610791498876
45. Marcsisin SR, Engen JR. Molecular insight into the conformational dynamics of the Elongin BC complex and its interaction with HIV-1 Vif. J Mol Biol 2010; 402:892-904; PMID:20728451; http://dx.doi.org/10.1016/j.jmb.2010.08.026
46. Bernacchi S, Henriet S, Dumas P, Paillart JC, Marquet R. RNA and DNA binding properties of HIV-1 Vif protein: a fluorescence study. J Biol Chem 2007; 282:26361-8; PMID:17609216; http://dx.doi.org/10.1074/jbc.M703122200
47. Bernacchi S, Mercenne G, Tournaire C, Marquet R, Paillart JC. Importance of the proline-rich multimerization domain on the oligomerization and nucleic acid binding properties of HIV-1 Vif. Nucleic Acids Res 2011; 39:2404-15; PMID:21076154; http://dx.doi.org/10.1093/nar/gkq979
48. Kuciak M, Gabus C, Ivanyi-Nagy R, Semrad K, Storchak R, Chaloin O, Muller S, Mély Y, Darlix JL. The HIV-1 transcriptional activator Tat has potent nucleic acid chaperoning activities in vitro. Nucleic Acids Res 2008; 36:3389-400; PMID:18442994; http://dx.doi.org/10.1093/nar/gkn177
49. Freisz S, Mezher J, Hafirassou L, Wolff P, Nominé Y, Romier C, Dumas P, Ennifar E. Sequence and structure requirements for specific recognition of HIV-1 TAR and DIS RNA by the HIV-1 Vif protein. RNA Biol 2012; 9:966-77; PMID:22767258; http://dx.doi.org/10.4161/rna.20483
50. Henriet S, Richer D, Bernacchi S, Decroly E, Vigne R, Ehresmann B, Ehresmann C, Paillart JC, Marquet R. Cooperative and specific binding of Vif to the 5′ region of HIV-1 genomic RNA. J Mol Biol 2005; 354:55-72; PMID:16236319; http://dx.doi.org/10.1016/j.jmb.2005.09.025
51. Dettenhofer M, Cen S, Carlson BA, Kleiman L, Yu XF. Association of human immunodeficiency virus type 1 Vif with RNA and its role in reverse transcription. J Virol 2000; 74:8938-45; PMID:10982337; http://dx.doi.org/10.1128/JVI.74.19.8938-8945.2000
52. Henriet S, Sinck L, Bec G, Gorelick RJ, Marquet R, Paillart JC. Vif is a RNA chaperone that could temporally regulate RNA dimerization and the early steps of HIV-1 reverse transcription. Nucleic Acids Res 2007; 35:5141-53; PMID:17660191; http://dx.doi.org/10.1093/nar/gkm542
53. Tisné C. Structural bases of the annealing of primer tRNA(3Lys) to the HIV-1 viral RNA. Curr HIV Res 2005; 3:147-56; PMID:15853720; http://dx.doi.org/10.2174/1570162053506919
54. Gabus C, Mazroui R, Tremblay S, Khandjian EW, Darlix JL. The fragile X mental retardation protein has nucleic acid chaperone properties. Nucleic Acids Res 2004; 32:2129-37; PMID:15096575; http://dx.doi.org/10.1093/nar/gkh535
55. Huvent I, Hong SS, Fournier C, Gay B, Tournier J, Carrière C, Courcoul M, Vigne R, Spire B, Boulanger P. Interaction and co-encapsidation of human immunodeficiency virus type 1 Gag and Vif recombinant proteins. J Gen Virol 1998; 79:1069-81; PMID:9603321
56. Khan MA, Akari H, Kao S, Aberham C, Davis D, Buckler-White A, Strebel K. Intravirion processing of the human immunodeficiency virus type 1 Vif protein by the viral protease may be correlated with Vif function. J Virol 2002; 76:9112-23; PMID:12186895; http://dx.doi.org/10.1128/JVI.76.18.9112-9123.2002
57. Yang X, Goncalves J, Gabuzda D. Phosphorylation of Vif and its role in HIV-1 replication. J Biol Chem 1996; 271:10121-9; PMID:8626571; http://dx.doi.org/10.1074/jbc.271.17.10121
58. Gallerano D, Devanaboyina SC, Swoboda I, Linhart B, Mittermann I, Keller W, Valenta R. Biophysical characterization of recombinant HIV-1 subtype C virus infectivity factor. Amino Acids 2011; 40:981-9; PMID:20809132; http://dx.doi.org/10.1007/s00726-010-0725-x
59. Techtmann SM, Ghirlando R, Kao S, Strebel K, Maynard EL. Hydrodynamic and functional analysis of HIV-1 Vif oligomerization. Biochemistry 2012; 51:2078-86; PMID:22369580; http://dx.doi.org/10.1021/bi201738a
60. Janes RW. Bioinformatics analyses of circular dichroism protein reference databases. Bioinformatics 2005; 21:4230-8; PMID:16188926; http://dx.doi.org/10.1093/bioinformatics/bti690
61. Tisné C, Roques BP, Dardel F. The annealing mechanism of HIV-1 reverse transcription primer onto the viral genome. J Biol Chem 2004; 279:3588-95; PMID:14602716; http://dx.doi.org/10.1074/jbc.M310368200
62. Tisné C, Rigourd M, Marquet R, Ehresmann C, Dardel F. NMR and biochemical characterization of recombinant human tRNA(Lys)3 expressed in Escherichia coli: identification of posttranscriptional nucleotide modifications required for efficient initiation of HIV-1 reverse transcription. RNA 2000; 6:1403-12; PMID:11073216; http://dx.doi.org/10.1017/S1355838200000947
63. Mély Y, de Rocquigny H, Sorinas-Jimeno M, Keith G, Roques BP, Marquet R, Gérard D. Binding of the HIV-1 nucleocapsid protein to the primer tRNA(3Lys), in vitro, is essentially not specific. J Biol Chem 1995; 270:1650-6; PMID:7829498; http://dx.doi.org/10.1074/jbc.270.4.1650
64. Tisné C, Roques BP, Dardel F. Heteronuclear NMR studies of the interaction of tRNA(Lys)3 with HIV-1 nucleocapsid protein. J Mol Biol 2001; 306:443-54; PMID:11178904; http://dx.doi.org/10.1006/jmbi.2000.4391
65. Paillart JC, Dettenhofer M, Yu XF, Ehresmann C, Ehresmann B, Marquet R. First snapshots of the HIV-1 RNA structure in infected cells and in virions. J Biol Chem 2004; 279:48397-403; PMID:15355993; http://dx.doi.org/10.1074/jbc.M408294200
66. Marquet R, Baudin F, Gabus C, Darlix JL, Mougel M, Ehresmann C, Ehresmann B. Dimerization of human immunodeficiency virus (type 1) RNA: stimulation by cations and possible mechanism. Nucleic Acids Res 1991; 19:2349-57; PMID:1645868; http://dx.doi.org/10.1093/nar/19.9.2349
67. Paillart JC, Marquet R, Skripkin E, Ehresmann B, Ehresmann C. Mutational analysis of the bipartite dimer linkage structure of human immunodeficiency virus type 1 genomic RNA. J Biol Chem 1994; 269:27486-93; PMID:7961663
68. Cruceanu M, Gorelick RJ, Musier-Forsyth K, Rouzina I, Williams MC. Rapid kinetics of protein-nucleic acid interaction is a major component of HIV-1 nucleocapsid protein's nucleic acid chaperone function. J Mol Biol 2006; 363:867-77; PMID:16997322; http://dx.doi.org/10.1016/j.jmb.2006.08.070
69. Bampi C, Bibillo A, Wendeler M, Divita G, Gorelick RJ, Le Grice SF, Darlix JL. Nucleotide excision repair and template-independent addition by HIV-1 reverse transcriptase in the presence of nucleocapsid protein. J Biol Chem 2006; 281:11736-43; PMID:16500895; http://dx.doi.org/10.1074/jbc.M600290200
70. Simon JH, Southerling TE, Peterson JC, Meyer BE, Malim MH. Complementation of vif-defective human immunodeficiency virus type 1 by primate, but not nonprimate, lentivirus vif genes. J Virol 1995; 69:4166-72; PMID:7769676
71. Etienne L, Hahn BH, Sharp PM, Matsen FA, Emerman M. Gene loss and adaptation to hominids underlie the ancient origin of HIV-1. Cell Host Microbe 2013; 14:85-92; PMID:23870316; http://dx.doi.org/10.1016/j.chom.2013.06.002
72. Tompa P. Intrinsically disordered proteins: a 10-year recap. Trends Biochem Sci 2012; 37:509-16; PMID:22989858; http://dx.doi.org/10.1016/j.tibs.2012.08.004

73. Kovacs D, Tompa P. Diverse functional manifestations of intrinsic structural disorder in molecular chaperones. Biochem Soc Trans 2012; 40:963-8; PMID:22988848; http://dx.doi.org/10.1042/BST20120108
74. Xue B, Mizianty MJ, Kurgan L, Uversky VN. Protein intrinsic disorder as a flexible armor and a weapon of HIV-1. Cell Mol Life Sci 2012; 69:1211-59; PMID:22033837; http://dx.doi.org/10.1007/s00018-011-0859-3
75. De Guzman RN, Wu ZR, Stalling CC, Pappalardo L, Borer PN, Summers MF. Structure of the HIV-1 nucleocapsid protein bound to the SL3 psi-RNA recognition element. Science 1998; 279:384-8; PMID:9430589; http://dx.doi.org/10.1126/science.279.5349.384
76. Paul I, Cui J, Maynard EL. Zinc binding to the HCCH motif of HIV-1 virion infectivity factor induces a conformational change that mediates protein-protein interactions. Proc Natl Acad Sci U S A 2006; 103:18475-80; PMID:17132731; http://dx.doi.org/10.1073/pnas.0604150103
77. Houzet L, Morichaud Z, Didierlaurent L, Muriaux D, Darlix JL, Mougel M. Nucleocapsid mutations turn HIV-1 into a DNA-containing virus. Nucleic Acids Res 2008; 36:2311-9; PMID:18296486; http://dx.doi.org/10.1093/nar/gkn069
78. Thomas JA, Bosche WJ, Shatzer TL, Johnson DG, Gorelick RJ. Mutations in human immunodeficiency virus type 1 nucleocapsid protein zinc fingers cause premature reverse transcription. J Virol 2008; 82:9318-28; PMID:18667500; http://dx.doi.org/10.1128/JVI.00583-08
79. Camaur D, Trono D. Characterization of human immunodeficiency virus type 1 Vif particle incorporation. J Virol 1996; 70:6106-11; PMID:8709234
80. Fouchier RA, Simon JH, Jaffe AB, Malim MH. Human immunodeficiency virus type 1 Vif does not influence expression or virion incorporation of gag-, pol-, and env-encoded proteins. J Virol 1996; 70:8263-9; PMID:8970945
81. Paillart JC, Skripkin E, Ehresmann B, Ehresmann C, Marquet R. In vitro evidence for a long range pseudoknot in the 5′-untranslated and matrix coding regions of HIV-1 genomic RNA. J Biol Chem 2002; 277:5995-6004; PMID:11744696; http://dx.doi.org/10.1074/jbc.M108972200
82. Dardel F. MC-Fit: using Monte-Carlo methods to get accurate confidence limits on enzyme parameters. Comput Appl Biosci 1994; 10:273-5; PMID:7922682
83. Piotto M, Saudek V, Sklenár V. Gradient-tailored excitation for single-quantum NMR spectroscopy of aqueous solutions. J Biomol NMR 1992; 2:661-5; PMID:1490109; http://dx.doi.org/10.1007/BF02192855
84. Weigelt J. Single scan, sensitivity- and gradient-enhanced TROSY for multidimensional NMR experiments. J Am Chem Soc 1998; 120:10778-9; http://dx.doi.org/10.1021/ja982649y
85. Ivanyi-Nagy R, Lavergne JP, Gabus C, Ficheux D, Darlix JL. RNA chaperoning and intrinsic disorder in the core proteins of Flaviviridae. Nucleic Acids Res 2008; 36:712-25; PMID:18033802; http://dx.doi.org/10.1093/nar/gkm1051
86. Andrade MA, Chacón P, Merelo JJ, Morán F. Evaluation of secondary structure of proteins from UV circular dichroism spectra using an unsupervised learning neural network. Protein Eng 1993; 6:383-90; PMID:8332596; http://dx.doi.org/10.1093/protein/6.4.383